Published in final edited form as:
Biomaterials. 2014 July ; 35(21): 5453–5461. doi:10.1016/j.biomaterials.2014.03.055.

Bone Regeneration using an Alpha 2 Beta 1 Integrin-Specific Hydrogel as a BMP-2 Delivery Vehicle

Asha Shekaran[1,2,4], **José R. García**[2,3], **Amy Y. Clark**[2,3], **Taylor E. Kavanaugh**[1], **Angela S. Lin**[2,3], **Robert E. Guldberg**[2,3], and **Andrés J. García**[2,3,*]

[1]Department of Biomedical Engineering, Georgia Institute of Technology and Emory University, 313 Ferst Drive, Atlanta, GA 30332, USA

[2]Petit Institute for Bioengineering and Biosciences, Georgia Institute of Technology, 315 Ferst Drive, Atlanta, GA 30332, USA

[3]School of Mechanical Engineering, Georgia Institute of Technology, 801 Ferst Drive, Atlanta, GA 30332, USA

Abstract

Non-healing bone defects present tremendous socioeconomic costs. Although successful in some clinical settings, bone morphogenetic protein (BMP) therapies require supraphysiological dose delivery for bone repair, raising treatment costs and risks of complications. We engineered a protease-degradable poly(ethylene glycol) (PEG) synthetic hydrogel functionalized with a triple helical, α2β1 integrin-specific peptide (GFOGER) as a BMP-2 delivery vehicle. GFOGER-functionalized hydrogels lacking BMP-2 directed human stem cell differentiation and produced significant enhancements in bone repair within a critical-sized bone defect compared to RGD hydrogels or empty defects. GFOGER functionalization was crucial to the BMP-2-dependent healing response. Importantly, these engineered hydrogels outperformed the current clinical carrier in repairing non-healing bone defects at low BMP-2 doses. GFOGER hydrogels provided sustained *in vivo* release of encapsulated BMP-2, increased osteoprogenitor localization in the defect site, enhanced bone formation and induced defect bridging and mechanically robust healing at low BMP-2 doses which stimulated almost no bone regeneration when delivered from collagen sponges. These findings demonstrate that GFOGER hydrogels promote bone regeneration in challenging defects with low delivered BMP-2 doses and represent an effective delivery vehicle for protein therapeutics with translational potential.

*To whom correspondence should be addressed. andres.garcia@me.gatech.edu.
[4]Current address: Bioprocessing Technology Institute, 20 Biopolis Way, #06-01 Centros, Singapore 138668

Author contributions: A.S. and A.J.G designed all experiments. A.S., T.E.K., J.R.G. and A.Y.C. performed research and performed data analysis. A.S.L. and R.E.G. provided critical input on μCT and mechanical testing. A.S. and A.J.G. wrote the paper and all co-authors edited the manuscript.

Competing interests: A.J.G., R.E.G., and A.S. are inventors on a patent for the use of integrin-specific ligands for regenerative medicine (US Patent 8,445,006 and pending divisional patent 13/372,234).

Keywords

Integrin-specific; Hydrogel; Polyethylene glycol; Bone healing; BMP-2; Protein delivery

Introduction

Over 1 million bone grafting, bone excision and fracture repair surgeries are performed annually in the US at a cost of approximately $5 billion [1–4]. While autografts are the gold standard therapy for non-healing bone defects, these grafts are limited by low availability as well as donor site pain and inflammation [5]. More recently, bone morphogenetic protein (BMP) therapies have emerged as promising alternatives to autografts and allografts. While BMP therapy has been successful in stimulating bone repair, the BMP doses used clinically are orders of magnitude higher [6] than physiological concentrations of BMP, resulting in high costs of treatment and complications such as ectopic bone formation, nerve injuries and inflammation [5, 7, 8, 9, 10]. Therefore, there is an unmet clinical need for improved BMP delivery vehicles which promote bone healing at low delivered BMP doses to enable safe, cost-effective and efficacious BMP treatments.

Hydrogels, water-swollen cross-linked polymer networks, offer tremendous advantages as vehicles for protein delivery due to their high cytocompatibility, low inflammatory profile, tailorable mechanics and biofunctionality, and injectable delivery method [11–13]. In particular, poly(ethylene glycol) (PEG) hydrogels are attractive because they resist non-specific protein adsorption, providing a ‘clean-slate’ background onto which desired biofunctionalities may be incorporated [14]. In addition, PEGs are widely used in FDA-approved therapeutic products as covalent modifiers of proteins and lipids [15], indicating a history of safety in patients. This has led to increasing research interest in delivering protein therapeutics such as BMP-2 and BMP-7 from synthetic and natural hydrogels to improve bone healing [16–19].

We have recently established PEG hydrogels cross-linked via maleimide groups as an alternative cross-linking chemistry to address limitations associated with other widely used PEG hydrogel polymerization chemistries such as free-radical polymerization [20]. The maleimide reactive group is extensively used in peptide bioconjugate chemistry because of its fast reaction kinetics and high specificity for thiols at physiological pH. Maleimide-based cross-linking of PEG hydrogels has significant advantages over other cross-linking chemistries, namely well-defined hydrogel structure, stoichiometric incorporation of bioligands, increased cytocompatibility, improved cross-linking efficiency, and reaction time scales appropriate for *in situ* gelation for *in vivo* applications [20]. Additionally, the base macromer exhibits minimal toxicity and inflammation *in vivo* and is rapidly excreted via the urine [21] – important considerations in establishing the safety and translational potential of these hydrogels.

A critical consideration in the design of protein delivery systems for regenerative medicine is the incorporation of extracellular matrix (ECM)-mimetic adhesive ligands. Many orthopaedic biomaterials utilize ECM-inspired peptides which promote integrin-ECM interactions to direct desired host cell responses [16, 22, 23] as these interactions regulate

cell survival, proliferation, migration and differentiation [24–26]. In particular, the interaction of α2β1 integrin with collagen I is a crucial signal for osteoblastic differentiation and mineralization [27–32]. The hexapeptide sequence Gly-Phe-Hyp-Gly-Glu-Arg (GFOGER), residues 502–507 of the α1(I) chain of type I collagen, serves as the major recognition site for α2β1 integrin binding [33–35]. Our group has previously engineered a synthetic collagen I-mimetic GFOGER-containing peptide, $GGYGGGP(GPP)_5GFOGER(GPP)_5GPC$, which recapitulates the triple helical structure of native collagen (Fig. S1) and binds α2β1 integrin with high affinity and specificity [36]. GFOGER peptide coatings on plastic, titanium and poly(caprolactone) support equivalent levels of α2β1 integrin-mediated cell adhesion as native collagen I [36], promote osteoblastic differentiation *in vitro* [22, 37], improve fixation of metal implants to rat cortices [22], and enhance bone healing in rat femur defects [38]. In contrast to the collagen I-mimetic GFOGER peptide, the widely used bioadhesive RGD peptides bind primarily to the αvβ3 integrin and do not have intrinsic osteogenic properties [39–41].

We hypothesized that presentation of the pro-osteogenic α2β1 integrin-specific GFOGER peptide to host cells combined with sustained release of low doses of BMP-2 would direct endogenous stem cell differentiation *in vivo* and promote bone healing. Therefore, we synthesized matrix metalloproteinase (MMP)-degradable PEG-maleimide hydrogels functionalized with GFOGER and incorporating recombinant human BMP-2. In order to test this hypothesis, we implanted protease-degradable GFOGER-modified PEG hydrogel BMP-2 carriers within critical-sized, non-healing murine radial bone defects in order to evaluate their effects on bone regeneration.

Materials and Methods

GFOGER-modified PEG hydrogel synthesis

GFOGER peptide, $GGYGGGP(GPP)_5GFOGER(GPP)_5GPC$ (Activotec), four-arm, maleimide-end functionalized (>95%) PEG macromer (PEG-MAL, 20 kDa, Laysan Bio), GRGDSPC (RGD adhesive peptide), and GCRDVPMSMRGGDRCG (VPM) cross-linker peptide (AAPTEC), and rhBMP-2 (R&D Biosystems) were used. 4% wt/v PEG-MAL hydrogels were synthesized by reacting PEG-MAL with adhesive peptides (RGD or GFOGER) followed by mixing in BMP-2 and VPM cross-linker at a volume ratio of 2:1:1:1 at the required concentrations to obtain the desired final concentrations of the adhesive peptide (0.5 – 2.0 mM) and BMP-2 (0.03, 0.06 or 0.3 μg per 1.5 μL hydrogel implant). The concentration of VPM used for the synthesis of each hydrogel was calculated to match the number of cysteine residues on the peptide cross-linker with the number of free (unreacted) maleimide groups remaining in the adhesive peptide-functionalized PEG-maleimide solution. The mixture of peptide-functionalized PEG-maleimide, BMP-2 and VPM cross-linker was incubated at 37 °C for 2–6 hours to allow for cross-linking before adding PBS to the hydrogels. For *in vitro* studies, thin gel discs were fabricated by covering polymerizing gel solutions with sterile Sigmacote-treated coverslips. For *in vivo* studies, hydrogel (1.5 μL) was cast within 4-mm long polyimide tube sleeves with laser machined 200 μm diameter holes to improve nutrient transport and cell invasion into the defect. All hydrogels used for *in vivo* studies contained 4% (wt/v) PEG-maleimide and 2.0 mM adhesive peptide. Collagen

sponges were cut with a 1 mm diameter biopsy sponge and placed within the polyimide sleeves, injected with a BMP-2 solution at an equivalent dose as was loaded in the GFOGER hydrogels and incubated for 10 minutes at room temperature to allow for adsorption to the collagen sponge prior to implantation.

In vitro assays

hMSCs (Lonza) were cultured in MSCGM (Lonza) and seeded (10,000 cells/cm^2) on hydrogel surfaces. Cells were cultured for up to 21 days in osteogenic media (Lonza). After 3 days of culture in osteogenic media, cells were incubated in 2 μM calcein and 4 μM ethidium homodimer for 30 minutes for Live/Dead staining and imaged on a Zeiss fluorescence microscope. At 14 days hMSCs were lysed and assayed for alkaline phosphatase activity (ALP) by incubating with MUP substrate. hMSCs were scraped in PBS, transferred to cold 50 mM Tris-HCl and sonicated to lyse the cells. The total protein content for each lysate sample was determined using a BCA assay kit (Thermo Scientific). Samples were diluted to the same total protein content before assaying for ALP. Samples and ALP standards were loaded into a 96-well plate, then incubated with MUP substrate at 37 °C for 1 hour and read at 360 nm excitation/465 nm emission. Mineral deposition at 21 days post-induction was assayed by Alizarin Red staining and extraction. Cells were fixed in 10% formalin, rinsed in water and incubated in 2% Alizarin Red solution for 20 minutes. After 4 washes in water, the stained cells were scraped in 10% acetic acid and heated to 85 °C for 10 minutes. The supernatant was collected after centrifugation, neutralized with 10% ammonium hydroxide and read at 405 nm.

Radial defect surgery

All animal experiments were performed with the approval of the Georgia Tech Animal Care and Use Committee with veterinary supervision and within the guidelines of the Guide for the Care and Use of Laboratory Animals. B6129SF2/J wild-type male mice (8–10 week old, Jackson Laboratories) were anesthetized under isoflurane, and fur was removed from the right forelimb. The forelimb was then swabbed with chlorohexidine and alcohol and a 1.5-cm incision was made in the skin. Muscle tissue overlying the ulna and radius were blunt dissected, and 2.5 mm defects were made in the right radius using a custom-machined bone cutter, while leaving the ulna intact. Hydrogel or collagen sponge placed within polyimide sleeves were implanted into the defect by fitting the sleeve over the radius at the proximal and distal ends of the defect, so that the hydrogel or collagen sponge filled the defect space. The incision was then closed with vicryl suture and wound clips. Mice were provided with a single dose of slow-release buprenorphine for pain relief and were monitored post-surgery for signs of distress, normal eating habits and movement.

BMP-2, GFOGER *in vivo* retention

GFOGER and BMP-2 were labeled with Vivotag 680 and Vivotag 800 IR dyes respectively. Labeled GFOGER and BMP-2 were incorporated into PEG hydrogels and implanted into mice as described earlier. GFOGER peptide and BMP-2 retention within the defect site (n=6) was analyzed by scanning mouse forelimbs (FMT 4000) on the 680 or 790 laser channels (Perkin Elmer, 1 mm source density, 65 source points per scan). The signal was

quantified by placing 3D regions of interest markers around the forelimb, using a 0 nM IR dye threshold and normalizing to the day 0 value.

Faxitron/μCT imaging and mechanical testing

Radial defects were imaged with the MX-20 Radiography System (Faxitron, 23kV energy setting, 15 s scan time). For μCT scanning, a 3.2 mm length of the radius centered around the 2.5 mm radial defects was scanned in anesthetized, live subjects using a VivaCT system (Scanco Medical, 145 μA intensity, 55 kVp energy, 200 ms integration time, and 15 μm resolution). Bone formation was evaluated by contouring 2D slices to include only the radius and applying a Gaussian filter (sigma = 1, support = 1, threshold = 540 mg HA/ccm). 3D μCT reconstructions display the full 3.2 mm length of radius scanned. However, in order to ensure that only new bone formation was measured, quantification of bone volume and mineral density within the defect was performed by evaluating only the middle 2.0 mm of defect.

Torsion to failure testing was performed on 8 week radial defects (n=5–9) as described [42] with modifications. The radii and ulnae were excised post-euthanasia, wrapped in PBS-soaked gauze and stored at −20 °C. On the day of testing, the bones were thawed and potted in woods-metal within potting blocks. After the ulna was cut, the potting blocks were tested using a Bose Electroforce ELF 3200 system. The radius was torqued to failure at a rate of 3 degrees per second and the torque was measured using a 0.07 N·m torque sensor (Transducer Techniques) (Fig. S3).

Histology and stem cell recruitment

For histology, bones were fixed in 10% neutral-buffered saline, decalcified and embedded in Immunobed or MMA. Sections (2 μm thick) were deplasticized and stained with Safranin-O/Fast Green. To quantify osteoprogenitor cell recruitment, radii were excised 7 days post-surgery. Cells were harvested by a 45 min collagenase I incubation of tissue and stained with anti-CD45 (FITC) and anti-CD 90 (APC) antibodies (Biolegend) and analyzed by flow cytometry (Accuri C6 cytometer, FlowJo software) to determine the proportion $CD45^{-}$/$CD90^{+}$ cells in the defect.

Statistical analyses

Error bars graphs represent SEM. Statistical comparisons between multiple groups were made by one-way ANOVA with post-hoc Tukey tests for parametric data, by Kruskal Wallis test with Dunn's post-hoc test for non-parametric data (bridging scores), and by t-test for comparisons of two groups in Graphpad. A $p < 0.05$ value was considered significant.

Results

Synthesis of GFOGER/BMP-2 hydrogels

We synthesized MMP-degradable, GFOGER-functionalized hydrogels with encapsulated BMP-2 in a facile two-step reaction (Fig 1). The terminal maleimide groups on the 4-armed PEG macromer (Fig 1A and B) underwent a Michael addition reaction with free sulfhydryl groups on the cysteine residues of the GFOGER peptide, resulting in a GFOGER-tethered

PEG-maleimide precursor (Fig 1B). The subsequent reaction of the GFOGER-functionalized PEG-maleimide macromer with a bi-cysteine cross-linking peptide (VPM) [43, 44], containing an MMP cleavage site, resulted in the formation of an insoluble cross-linked PEG hydrogel network (Fig 1B). In this modular system, BMP-2 can be incorporated into the hydrogel by physical entrapment during network cross-linking. In the presence of cell-secreted proteases, the VPM cross-linker is cleaved, disrupting the PEG network and releasing the entrapped BMP-2 (Fig 1B). We chose a peptide cross-linker which undergoes rapid degradation in response to MMP in order to tailor the *in vivo* degradation rate of the PEG hydrogels to obtain a half-life of 1–2 weeks. To determine the efficiency at which GFOGER ligand was covalently tethered to PEG-maleimide, we measured the free sulfhydryl groups in reaction mixtures of GFOGER and PEG-maleimide at varying maleimide:GFOGER molar ratios. At a molar ratio higher than 5, ~ 100% of added GFOGER was tethered to PEG-maleimide (Fig S2), providing precise control of GFOGER density within the hydrogel.

In vitro cell activities on engineered hydrogels

We first evaluated the potential of GFOGER-functionalized PEG hydrogels to direct osteoblastic differentiation in human mesenchymal stem cells (hMSCs). GFOGER-functionalized hydrogels were compared to hydrogels modified with RGD peptides as RGD is the most commonly used adhesive peptide in the biomaterials field. We tested the levels of *in vitro* osteoblastic differentiation of hMSCs cultured on hydrogel surfaces. GFOGER- and RGD-functionalized hydrogels supported dose-dependent levels of hMSC adhesion and spreading (Fig 2A), while significantly fewer cells adhered to PEG-only (no ligand) gels or scrambled RDG peptide-modified gels and these cells remained rounded (Fig 2A). hMSCs exhibited high viability on both GFOGER- and RGD-tethered hydrogels at 3 days in culture (Fig 2B). Despite comparable levels of adhesion and viability on GFOGER- and RGD-functionalized gels, hMSCs on GFOGER-functionalized hydrogels exhibited 94% and 40% increases in alkaline phosphatase activity and Alizarin Red staining, respectively, compared to RGD-presenting gels (Fig 2C).

Repair of non-healing bone defects

We evaluated the potential of GFOGER-functionalized hydrogels to promote bone repair in a murine non-healing radial bone defect model [45]. If left untreated, this critical-sized defect does not heal over the experimental period and provides a stringent bone repair model analogous to non-healing, long bone defects in humans. To improve the ease of handling, we pre-cast hydrogels within polyimide tube sleeves. The sleeve walls were laser machined with holes to improve nutrient transport and cell migration across the sleeve walls as including perforations within a mesh sleeve surrounding a BMP-containing hydrogel has been shown to improve healing outcomes [46]. We implanted hydrogel constructs into 2.5 mm-long unilateral murine radial critical-sized defects (Fig 2D) and evaluated bone healing by radiography and microcomputed tomography (μCT) at 4 and 8 weeks post-surgery. Defects treated with GFOGER-functionalized hydrogels exhibited significantly improved bone healing compared to those treated with no hydrogel (defects received an empty polyimide sleeve implant) and RGD-modified gel implants (Fig 2E–H). Bone volume at 8 weeks for defects treated with GFOGER-functionalized gel was 140% and 150% higher

than no hydrogel and RGD-presenting gel-treated defects, respectively (Fig 2F, G). There was no difference in bone volume between RGD-modified gels and empty defects. Furthermore, while minimal bone formation and no defect bridging was observed in all subjects treated with RGD-functionalized gel and empty defect controls, several defects treated with GFOGER-functionalized hydrogels were close to full bridging after 8 weeks (Fig 2E–F). We scored the degree to which defects were bridged 8 weeks after implantation according to the following criteria: 0 - defect is less than half bridged, 1 - defect is more than half bridged, and 2 - defect is fully bridged. Bridging scores for GFOGER-functionalized hydrogels were higher than RGD-presenting gels and empty defects (Fig 2H). These results demonstrate that α2β1 integrin-specific GFOGER-functionalized hydrogels promote hMSC osteogenic differentiation and enhance bone repair compared to conventional RGD-tethered gels or treatment with no hydrogel.

Dose response of BMP-2 in hydrogels in bone repair

Because GFOGER-modified PEG hydrogels supported great enhancements in bone healing, we explored whether combining GFOGER gels with low doses of BMP-2 could yield further improvements in bone healing and bridge critical-sized segmental defects. Five groups were tested: implants containing no hydrogel (empty sleeve) as a negative control and GFOGER-functionalized hydrogels lacking BMP-2 (0 μg) or incorporating increasing BMP-2 doses (0.03, 0.06 and 0.3 μg, referred to as low, medium and high doses respectively). There was minimal bone healing in defects treated with no hydrogel and high levels of bone formation and almost complete bridging with treatment with GFOGER-functionalized hydrogels without BMP-2 (Fig 3A–D). For the medium and high BMP-2 doses, defect bridging was observed by week 4 (Fig 3B (i)), and for all BMP-2 doses, bone volumes were increased compared to no hydrogel implants, and bridging occurred by week 8 (Fig 3A–C). Even within defects treated with the low BMP-2 dose, bone volume was 200% higher than defects which received no hydrogel (Fig 3C). Treatment with all GFOGER-functionalized hydrogels including those lacking BMP-2 resulted in increased bridging scores compared to the no hydrogel treatment (Fig 3D). Histological analysis revealed that PEG hydrogels were completely degraded by week 8, facilitating cell invasion into the defects (Fig 3E). In addition, non-woven bone containing marrow compartments was formed in defects treated with GFOGER-functionalized hydrogels but not in the no hydrogel group (Fig 3E). Importantly, low dose BMP-2 treatment within GFOGER-functionalized hydrogels induced bone defect bridging after 8 weeks without any structural change to the adjacent ulna (Fig 3B (ii)). In mice receiving implants with the medium and high BMP-2 doses, radial defect bridging also occurred, but was accompanied by unintended alterations to the ulna (Fig 3B (ii)). Treatment with medium dose-BMP-2 resulted in expansion of the ulna around the radius, while for the high dose BMP-2 group, the ulna completely encircled the radius and fused with the radius (Fig 3B (ii)). These results highlight the adverse effects of excessive BMP-2 delivery, recapitulating off-target clinical results in humans [47], and underscore the importance of precise control of the dose and release mechanism of BMP-2.

Because BMP-2 release kinetics as well as scaffold degradation and cell invasion are important factors which contribute to tissue healing in response to implantable biomaterials,

we examined the retention times of near infrared (IR) dye-labeled GFOGER peptide and BMP-2 in PEG hydrogels within the radial defect site using fluorescence molecular tomography (FMT). BMP-2 was localized within the defect site over a prolonged period of time (Fig 3F). The half-life for BMP-2 was 5.65 days and more than 20% of the initial BMP-2 dose remained 14 days after surgery, indicating sustained release of BMP-2 from GFOGER hydrogels *in vivo* (Fig 3F (ii)). The half-life of GFOGER peptide within the defect site was considerably longer than BMP-2 at 11.0 days and is an indication of the retention time of the bulk PEG polymer to which the peptide was tethered (Fig D (iii)). This result confirms our targeted *in vivo* hydrogel degradation rate of 1–2 week half-life using the MMP-cleavable VPM cross-linker. Because GFOGER-functionalized hydrogels incorporating low-dose BMP-2 supported localized bone formation and bridging within the radial defect without inducing any off-target alterations to bone volume or structure in the ulna, we used GFOGER gels with low BMP-2 dose (GFOGER/low BMP-2) delivery in subsequent analyses.

Contributions of GFOGER and BMP-2 to bone healing

A major advantage of the PEG-maleimide hydrogel platform is the ability to independently control its modular components to examine their relative contributions to tissue repair. We therefore systematically tested combinations of implants containing GFOGER peptide, low BMP-2 dose, or the combination of both. Four groups were tested (Fig 4A): GFOGER/low BMP-2 (PEG/GFOGER/BMP-2), GFOGER/no BMP-2 (PEG/GFOGER), no ligand/low dose BMP-2 (PEG/BMP-2), and no ligand/noBMP-2 (PEG). GFOGER/low BMP-2 hydrogels supported robust healing and defect bridging within 8 weeks, while GFOGER/no BMP-2 gels induced significant bone formation and almost complete bridging (Fig 4B–D, S2). GFOGER/low BMP-2 gels displayed enhancements in bone volume, defect bridging and maximum torque compared to groups lacking GFOGER (Fig 4B–E). BMP-containing implants that lacked GFOGER (no ligand/low dose BMP-2) gels supported no defect bridging and exhibited ~70% lower bone volume than GFOGER/low dose BMP-2 gels and 30% less bone volume than GFOGER/no BMP-2 gels (Fig 4C), indicating that the GFOGER peptide is critical to the bone repair activity of the engineered hydrogel. Taken together, these results demonstrate that GFOGER is critical to bone repair and BMP-2 further enhances the osseoreparative properties of these hydrogels.

Bone repair and osteoprogenitor recruitment compared to the standard carrier

In current clinical practice, BMP-2 is delivered by injecting a BMP-2 solution into collagen foams prior to implantation. Therefore, in order to compare our engineered biomaterial to the clinical standard, we examined the role of the delivery vehicle on bone formation in response to 0.03 μg BMP-2 dose, the lowest dose tested in the dose-response study. Two groups were compared: GFOGER hydrogels and collagen sponges loaded with 0.03 μg BMP-2. μCT evaluation of bone volume within defects revealed that GFOGER/BMP-2 hydrogel implants improved bone healing compared to collagen sponge/BMP-2 implants by 200% and >300% at 4 and 8 weeks, respectively (Fig 5A, B). Defects treated with GFOGER/BMP-2 hydrogels bridged consistently, whereas collagen sponge/BMP-2 treated defects exhibited minimal bone healing (Fig 5A, B) with no bridging (Fig 5C). Importantly, GFOGER/BMP-2 treated defects were mechanically robust and showed a 100% increase in

maximum torque at 8 weeks compared to defects treated with collagen sponge/BMP-2 (Fig 5D). Notably, the maximum torque levels for the defects treated with GFOGER/BMP-2 were equivalent to the maximum torque of intact radii (3.2 ± 0.3 mN·m), demonstrating that the quality of the repair tissue is similar to native bone. Histological analysis at 8 weeks showed fibrous tissue with almost no bone tissue formation for collagen sponge/BMP-2, whereas defects treated with GFOGER/BMP-2 hydrogels exhibited abundant bone formation as well as establishment of bone marrow in the center of the defect (Fig 5E). Both the collagen sponge and PEG hydrogel were fully degraded by 8 weeks after implantation (Fig 5E).

Because BMP-2 release kinetics greatly impact bone healing, we compared the release rates of BMP-2 from GFOGER gels and collagen sponges in the bone defect using Vivotag800-labeled BMP-2. GFOGER-functionalized hydrogels exhibited 30% higher levels of BMP-2 retained within the radial defect space at 1 day and 90% higher levels at 5 days post-implantation compared to the collagen sponge (Fig 5F) by fluorescence molecular tomography. Because BMP-2 is known to have chemotactic effects on mesenchymal stem cells and osteoprogenitor cells [48], we evaluated the recruitment of $CD45^{-}/CD90^{+}$ osteoprogenitor stem cells to the defect site following the implantation of GFOGER/BMP-2 hydrogels or collagen sponge/BMP-2 (Fig 5G). At 7 days post-implantation, there was a 300% increase in $CD45^{-}/CD90^{+}$ cells in defects treated with GFOGER/BMP-2 gels compared to collagen/BMP-2 (Fig 5G). These results demonstrate that GFOGER-functionalized PEG hydrogels delivering BMP-2 outperform the current clinical standard delivery vehicle in terms of bone repair and provide sustained release of BMP-2 and enhanced osteoprogenitor stem cell recruitment.

Discussion

Bone grafts are widely used in clinical practice for spinal, foot and ankle fusions, revision arthroplasties, and treating large, non-healing bone defects. Because the gold-standard autograft treatments cause donor pain and are in limited supply [5] and processed allografts exhibit limited bioactivity or risks of infection [2, 5, 49, 50], protein therapeutics are becoming extensively used in the clinic. However, BMP treatments present cost limitations [7] and clinical safety concerns [5, 8–10], primarily because suboptimal growth factor carriers require BMP to be delivered at supraphysiological doses. Therefore, there is a strong motivation to engineer protein therapeutic delivery systems which offer greater safety and cost-effectiveness by reducing the therapeutic dose of growth factors required for healing of critical sized bone defects.

Here, we engineered a hydrogel carrier functionalized with a collagen-mimetic, triple helical, integrin-specific peptide (GFOGER) which significantly enhanced bone healing compared to collagen sponges, the current clinical BMP-2 carrier. GFOGER-modified gels incorporating low doses of BMP-2 promoted osteoprogenitor cell recruitment to the defect site and produced robust repair and bridging of segmental bone defects within 8 weeks. Importantly, the repair tissue had equivalent mechanical strength to native bone. Furthermore, this result was achieved with GFOGER gels loaded with a low dose of BMP-2 which supported almost no bone formation within clinical standard collagen foam vehicles.

These results show that GFOGER- gels produce superior healing outcomes compared to current carriers for protein therapeutics. Follow-up studies with large animal models are required to fully establish the translational potential of these delivery vehicles.

The improved healing induced by the GFOGER-tethered PEG gels compared to collagen foams can be attributed to a combination of factors. First, in contrast to collagen foams [51], GFOGER-functionalized materials enhance bone formation without cell or protein co-delivery due to the intrinsic osteogenic bioactivity of the α2β1 integrin-specific GFOGER peptide. Simple presentation of GFOGER within the hydrogel significantly enhanced bone formation, outperforming other adhesive peptides such as RGD. Second, GFOGER gels provided sustained release of encapsulated BMP-2 compared to the clinical collagen sponge carrier. This improvement in BMP-2 release kinetics from GFOGER gels is due to effective entrapment of BMP-2 within the tightly cross-linked hydrogel network and MMP-dependent gel degradation. In contrast, collagen foams have large micron-scale pores and release BMP-2 through protein desorption from scaffold surfaces, diffusion of BMP-2 from solution trapped in the pores, and collagenase-mediated degradation of the foams. Third, GFOGER-functionalized hydrogels support rapid MMP-mediated hydrogel degradation and cell invasion that allows for replacement of the carrier with repair tissue. Indeed, we demonstrated a 3-fold enhancement in the recruitment of osteoprogenitor cells for GFOGER gels compared to collagen sponges.

The α2β1 integrin-specific PEG hydrogel BMP-2 carrier described in this study has potential for clinical translation because it demonstrates superior bone healing compared to the commonly used adhesive RGD peptide and collagen sponges and is a purely synthetic, well tolerated, and tunable system. GFOGER gels supported 150% more bone formation than RGD gels. Notably, the well-defined, synthetic nature of the GFOGER-functionalized PEG hydrogel carrier makes it amenable to scale-up in production and well-regulated quality control. Furthermore, the modularity of the PEG-maleimide hydrogels allows key properties such as degradation rate as well as the density or combinations of adhesive ligands and therapeutic proteins to be tuned to optimize or adapt the material for other applications.

Conclusion

This study highlights the bone regeneration potential of a synthetic PEG-maleimide hydrogel functionalized with the α2β1 integrin-specific GFOGER peptide as a BMP-2 carrier. GFOGER-functionalized hydrogels displayed intrinsic osteogenic activity, provided sustained release of BMP-2, underwent rapid degradation *in vivo*, bridged critical-sized bone defects at low BMP-2 doses, and exhibited improved bone repair compared to the collagen foams which are the clinical standard carriers. These findings underscore the effectiveness of targeting pro-osteogenic integrins to enhance bone regeneration and establish the GFOGER-modified PEG-maleimide hydrogel as an effective BMP-2 delivery vehicle with significant translational potential.

Supplementary Material

Refer to Web version on PubMed Central for supplementary material.

Acknowledgments

We thank Ningtao Cheng for his assistance with mechanical testing and Aby Thyparambil and Robert Latour at Clemson University for CD analysis. The facilities at Clemson University were supported by NIH Grants 5P20RR021949 and 8P20GM103444. This work was funded by the USA National Institutes for Health (R01 AR062920, R01 AR062368). A.S. was supported by the Singaporean Agency for Science, Technology and Research.

References

1. Bucholz RW. Nonallograft osteoconductive bone graft substitutes. Clin Orthop Relat Res. 2002; 395:44–52. [PubMed: 11937865]
2. Finkemeier CG. Bone-grafting and bone-graft substitutes. J Bone Joint Surg Am. 2002; 84-A(3): 454–64. [PubMed: 11886919]
3. Giannoudis PV, Dinopoulos H, Tsiridis E. Bone substitutes: an update. Injury. 2005; 36 (Suppl 3):S20–7. [PubMed: 16188545]
4. Kretlow JD, Mikos AG. Review: mineralization of synthetic polymer scaffolds for bone tissue engineering. Tissue Eng. 2007; 13(5):927–38. [PubMed: 17430090]
5. De Long WG Jr, Einhorn TA, Koval K, McKee M, Smith W, Sanders R, et al. Bone grafts and bone graft substitutes in orthopaedic trauma surgery. A critical analysis. J Bone Joint Surg Am. 2007; 89(3):649–58. [PubMed: 17332116]
6. Schmidmaier G, Schwabe P, Strobel C, Wildemann B. Carrier systems and application of growth factors in orthopaedics. Injury. 2008; 39 (Suppl 2):S37–43. [PubMed: 18804572]
7. Desai BM. Osteobiologics. Am J Orthop (Belle Mead NJ). 2007; 36(4 Suppl):8–11. [PubMed: 17547352]
8. Carragee EJ, Hurwitz EL, Weiner BK. A critical review of recombinant human bone morphogenetic protein-2 trials in spinal surgery: emerging safety concerns and lessons learned. Spine J. 2011; 11(6):471–91. [PubMed: 21729796]
9. Yoon ST, Boden SD. Osteoinductive molecules in orthopaedics: basic science and preclinical studies. Clin Orthop Relat Res. 2002; (395):33–43. [PubMed: 11937864]
10. Bishop GB, Einhorn TA. Current and future clinical applications of bone morphogenetic proteins in orthopaedic trauma surgery. Int Orthop. 2007; 31(6):721–7. [PubMed: 17668207]
11. Mikos AG, Herring SW, Ochareon P, Elisseeff J, Lu HH, Kandel R, et al. Engineering complex tissues. Tissue Eng. 2006; 12(12):3307–39. [PubMed: 17518671]
12. Salinas CN, Anseth KS. Mesenchymal stem cells for craniofacial tissue regeneration: designing hydrogel delivery vehicles. J Dent Res. 2009; 88(8):681–92. [PubMed: 19734453]
13. Lutolf MP, Hubbell JA. Synthetic biomaterials as instructive extracellular microenvironments for morphogenesis in tissue engineering. Nat Biotechnol. 2005; 23(1):47–55. [PubMed: 15637621]
14. Ratner, BD.; Hoffman, AS. Non-Fouling Surfaces. In: Buddy, DR.; Allan, SH.; Frederick, JS.; Jack, EL., editors. Biomaterials Science: An Introduction to Materials in Medicine. 3. Academic Press; 2013. p. 241-7.
15. Bailon P, Won CY. PEG-modified biopharmaceuticals. Expert Opin Drug Deliv. 2009; 6(1):1–16. [PubMed: 19236204]
16. Lutolf MP, Weber FE, Schmoekel HG, Schense JC, Kohler T, Muller R, et al. Repair of bone defects using synthetic mimetics of collagenous extracellular matrices. Nat Biotechnol. 2003; 21(5):513–8. [PubMed: 12704396]
17. Mariner PD, Wudel JM, Miller DE, Genova EE, Streubel SO, Anseth KS. Synthetic hydrogel scaffold is an effective vehicle for delivery of INFUSE (rhBMP2) to critical-sized calvaria bone defects in rats. J Orthop Res. 2013; 31(3):401–6. [PubMed: 23070779]

18. Reichert JC, Cipitria A, Epari DR, Saifzadeh S, Krishnakanth P, Berner A, et al. A tissue engineering solution for segmental defect regeneration in load-bearing long bones. Sci Transl Med. 2012; 4(141):141ra93.
19. Boerckel JD, Kolambkar YM, Dupont KM, Uhrig BA, Phelps EA, Stevens HY, et al. Effects of protein dose and delivery system on BMP-mediated bone regeneration. Biomaterials. 2011; 32(22):5241–51. [PubMed: 21507479]
20. Phelps EA, Enemchukwu NO, Fiore VF, Sy JC, Murthy N, Sulchek TA, et al. Maleimide cross-linked bioactive PEG hydrogel exhibits improved reaction kinetics and cross-linking for cell encapsulation and in situ delivery. Adv Mater. 2012; 24(1):64–70. 2. [PubMed: 22174081]
21. Phelps EA, Headen DM, Taylor WR, Thule PM, Garcia AJ. Vasculogenic bio-synthetic hydrogel for enhancement of pancreatic islet engraftment and function in type 1 diabetes. Biomaterials. 2013; 34(19):4602–11. [PubMed: 23541111]
22. Reyes CD, Petrie TA, Burns KL, Schwartz Z, Garcia AJ. Biomolecular surface coating to enhance orthopaedic tissue healing and integration. Biomaterials. 2007; 28(21):3228–35. [PubMed: 17448533]
23. Martino MM, Tortelli F, Mochizuki M, Traub S, Ben-David D, Kuhn GA, et al. Engineering the growth factor microenvironment with fibronectin domains to promote wound and bone tissue healing. Sci Transl Med. 2011; 3(100):100ra89.
24. Bourdoulous S, Orend G, MacKenna DA, Pasqualini R, Ruoslahti E. Fibronectin matrix regulates activation of RHO and CDC42 GTPases and cell cycle progression. J Cell Biol. 1998; 143(1):267–76. [PubMed: 9763437]
25. Chen CS, Mrksich M, Huang S, Whitesides GM, Ingber DE. Geometric control of cell life and death. Science. 1997; 276(5317):1425–8. [PubMed: 9162012]
26. Giancotti FG, Ruoslahti E. Integrin signaling. Science. 1999; 285(5430):1028–32. [PubMed: 10446041]
27. Mizuno M, Fujisawa R, Kuboki Y. Type I collagen-induced osteoblastic differentiation of bone-marrow cells mediated by collagen-alpha 2 beta 1 integrin interaction. J Cell Physiol. 2000; 184(2):207–13. [PubMed: 10867645]
28. Jikko A, Harris SE, Chen D, Mendrick DL, Damsky CH. Collagen integrin receptors regulate early osteoblast differentiation induced by BMP-2. J Bone Miner Res. 1999; 14(7):1075–83. [PubMed: 10404007]
29. Mizuno M, Kuboki Y. Osteoblast-related gene expression of bone marrow cells during the osteoblastic differentiation induced by type I collagen. J Biochem. 2001; 129(1):133–8. [PubMed: 11134967]
30. Suzawa M, Tamura Y, Fukumoto S, Miyazono K, Fujita T, Kato S, et al. Stimulation of Smad1 transcriptional activity by Ras-extracellular signal-regulated kinase pathway: a possible mechanism for collagen-dependent osteoblastic differentiation. J Bone Miner Res. 2002; 17(2): 240–8. [PubMed: 11811554]
31. Takeuchi Y, Suzawa M, Kikuchi T, Nishida E, Fujita T, Matsumoto T. Differentiation and transforming growth factor-beta receptor down-regulation by collagen-alpha2beta1 integrin interaction is mediated by focal adhesion kinase and its downstream signals in murine osteoblastic cells. J Biol Chem. 1997; 272(46):29309–16. [PubMed: 9361011]
32. Xiao G, Wang D, Benson MD, Karsenty G, Franceschi RT. Role of the alpha2-integrin in osteoblast-specific gene expression and activation of the Osf2 transcription factor. J Biol Chem. 1998; 273(49):32988–94. [PubMed: 9830051]
33. Morton LF, Peachey AR, Zijenah LS, Goodall AH, Humphries MJ, Barnes MJ. Conformation-dependent platelet adhesion to collagen involving integrin alpha 2 beta 1-mediated and other mechanisms: multiple alpha 2 beta 1-recognition sites in collagen type I. Biochem J. 1994; 299 (Pt 3):791–7. [PubMed: 7514871]
34. Knight CG, Morton LF, Peachey AR, Tuckwell DS, Farndale RW, Barnes MJ. The collagen-binding A-domains of integrins alpha(1)beta(1) and alpha(2)beta(1) recognize the same specific amino acid sequence, GFOGER, in native (triple-helical) collagens. J Biol Chem. 2000; 275(1): 35–40. [PubMed: 10617582]

35. Knight CG, Morton LF, Onley DJ, Peachey AR, Messent AJ, Smethurst PA, et al. Identification in collagen type I of an integrin alpha2 beta1-binding site containing an essential GER sequence. J Biol Chem. 1998; 273(50):33287–94. [PubMed: 9837901]
36. Reyes CD, Garcia AJ. Engineering integrin-specific surfaces with a triple-helical collagen-mimetic peptide. J Biomed Mater Res A. 2003; 65(4):511–23. [PubMed: 12761842]
37. Reyes CD, Garcia AJ. Alpha2beta1 integrin-specific collagen-mimetic surfaces supporting osteoblastic differentiation. J Biomed Mater Res A. 2004; 69(4):591–600. [PubMed: 15162400]
38. Wojtowicz AM, Shekaran A, Oest ME, Dupont KM, Templeman KL, Hutmacher DW, et al. Coating of biomaterial scaffolds with the collagen-mimetic peptide GFOGER for bone defect repair. Biomaterials. 2010; 31(9):2574–82. [PubMed: 20056517]
39. Miljkovic ND, Cooper GM, Hott SL, Disalle BF, Gawalt ES, Smith DM, et al. Calcium aluminate, RGD-modified calcium aluminate, and beta-tricalcium phosphate implants in a calvarial defect. J Craniofac Surg. 2009; 20(5):1538–43. [PubMed: 19816293]
40. Hennessy KM, Clem WC, Phipps MC, Sawyer AA, Shaikh FM, Bellis SL. The effect of RGD peptides on osseointegration of hydroxyapatite biomaterials. Biomaterials. 2008; 29(21):3075–83. [PubMed: 18440064]
41. Jager M, Boge C, Janissen R, Rohrbeck D, Hulsen T, Lensing-Hohn S, et al. Osteoblastic potency of bone marrow cells cultivated on functionalized biometals with cyclic RGD-peptide. J Biomed Mater Res A. 2013
42. Duvall CL, Taylor WR, Weiss D, Wojtowicz AM, Guldberg RE. Impaired angiogenesis, early callus formation, and late stage remodeling in fracture healing of osteopontin-deficient mice. J Bone Miner Res. 2007; 22(2):286–97. [PubMed: 17087627]
43. Patterson J, Hubbell JA. SPARC-derived protease substrates to enhance the plasmin sensitivity of molecularly engineered PEG hydrogels. Biomaterials. 2011; 32(5):1301–10. [PubMed: 21040970]
44. Patterson J, Hubbell JA. Enhanced proteolytic degradation of molecularly engineered PEG hydrogels in response to MMP-1 and MMP-2. Biomaterials. 2010; 31(30):7836–45. [PubMed: 20667588]
45. Kimelman-Bleich N, Pelled G, Zilberman Y, Kallai I, Mizrahi O, Tawackoli W, et al. Targeted gene-and-host progenitor cell therapy for nonunion bone fracture repair. Mol Ther. 2011; 19(1): 53–9. [PubMed: 20859259]
46. Kolambkar YM, Boerckel JD, Dupont KM, Bajin M, Huebsch N, Mooney DJ, et al. Spatiotemporal delivery of bone morphogenetic protein enhances functional repair of segmental bone defects. Bone. 2011; 49(3):485–92. [PubMed: 21621027]
47. Lehman RA Jr, Kang DG. Symptomatic ectopic intracanal ossification after transforaminal lumbar interbody fusion with rhBMP-2. Spine J. 2012; 12(6):530–1. [PubMed: 22682741]
48. Fiedler J, Roderer G, Gunther KP, Brenner RE. BMP-2, BMP-4, and PDGF-bb stimulate chemotactic migration of primary human mesenchymal progenitor cells. J Cell Biochem. 2002; 87(3):305–12. [PubMed: 12397612]
49. Sorger JI, Hornicek FJ, Zavatta M, Menzner JP, Gebhardt MC, Tomford WW, et al. Allograft fractures revisited. Clin Orthop Relat Res. 2001; (382):66–74. [PubMed: 11154007]
50. Mankin HJ, Hornicek FJ, Raskin KA. Infection in massive bone allografts. Clin Orthop Relat Res. 2005; (432):210–6. [PubMed: 15738824]
51. Azad V, Breitbart E, Al-Zube L, Yeh S, O'Connor JP, Lin SS. rhBMP-2 enhances the bone healing response in a diabetic rat segmental defect model. J Orthop Trauma. 2009; 23(4):267–76. [PubMed: 19318870]

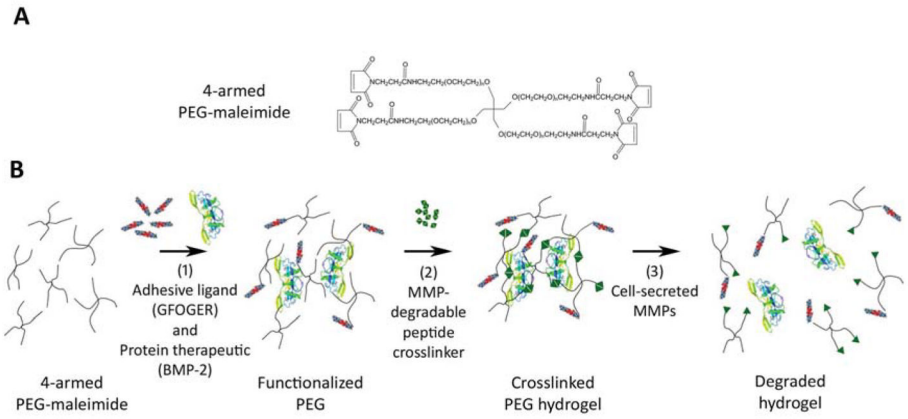

Fig. 1.

Protease-degradable integrin-specific GFOGER-modified PEG hydrogels are synthesized with precise control of GFOGER density. (A) Chemical structure of branched 4-armed PEG-maleimide. (B) Synthesis of GFOGER- and BMP-2-functionalized hydrogels.

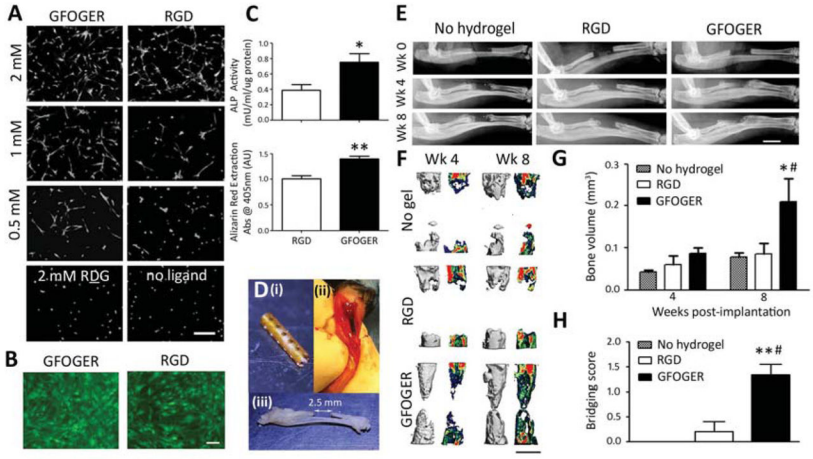

Fig. 2.

GFOGER-functionalized hydrogels promote differentiation and bone healing. (A) Calcein-stained hMSCs on GFOGER- and RGD-tethered gels at varying densities ofligand and non-adhesive controls 1 day after seeding, scale bar 50 μm, n=3. (B) Live/Dead stained hMSCs on 2.0 mM GFOGER- and 2.0 mM RGD-presenting hydrogels 3 days after osteogenic induction, scale bar 20 μm, n=3. (C) ALP activity at 14 days, n=4 (top) and Alizarin Red stain for mineralization of hMSCs at 21 days, n=4 (bottom). Hydrogels were pre-cast in a polyimide sleeve with 200 μm diameter holes along tube walls. (D) Pictures indicate (i) a polyimide tube sleeve, (ii) radial defect with hydrogel-sleeve implant, hydrogel stained blue, and (iii) excised radius and ulna with 2.5 mm radial defect (iii). (E) Radiographic images of radial defects treated with hydrogel, scale bar 2 mm. (F) 3D μCT reconstructions (left) and mineral density mappings on sagittal sections of the defects (right), scale bar 1 mm, n=5–6. (G) μCT measures of bone volume within defects, n=5–6. (H) Bridging scores for defects receiving implants containing no hydrogel, or hydrogels functionalized with RGD or GFOGER, n=5–6, 0 – < half bridged, 1- > half bridged, 2 – completely bridged - 8 weeks post-surgery. *p<0.05, **p<0.01 compared to RGD, #p<0.05, ##p<0.01 compared to No hydrogel.

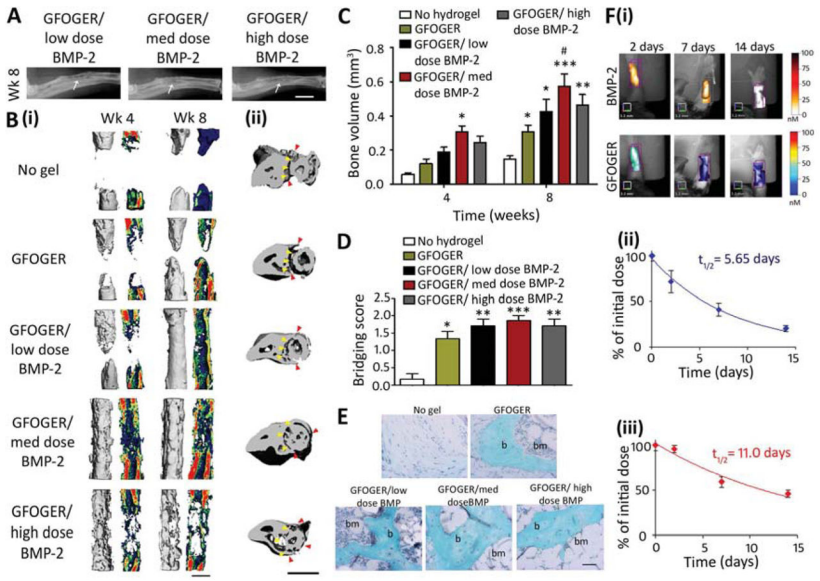

Fig. 3.

GFOGER-functionalized PEG hydrogels with low-dose BMP-2 bridge radial segmental defects without altering ulnar structure. (A) Radiographic images, white arrows indicate space between ulna and radius which is not present in the high BMP-2 dose image, scale bar 2 mm. (B) 3D μCT reconstructions of (i) radius in sagittal view (left) with mineral density mapping (right), and (ii) radius and ulna in transverse view. Yellow arrowheads indicate boundary between the ulna and radius prior to implantation, red arrowheads indicate the position of the ulna closest to the radius at 8 weeks, scale bar 1 mm. (C) μCT measures of bone formation, n=6–7. (D) Scoring of defect bridging at 8 weeks, n=6–7. (E) Sections stained with Safranin O/Fast Green at the center of defect, scale bar 50 μm. b - bone, bm - bone marrow. (F) (i) Representative FMT images and FMT quantification of % implanted dose retained in radial defect space over time *in vivo* for (ii) high dose BMP-2 labeled with Vivotag 800 and (iii) GFOGER peptide labeled with Vivotag 680, n=6. * $p<0.05$, ** $p<0.01$, *** $p<0.001$ compared to defect receiving no hydrogel implant, # $p<0.05$ compared to GFOGER hydrogel.

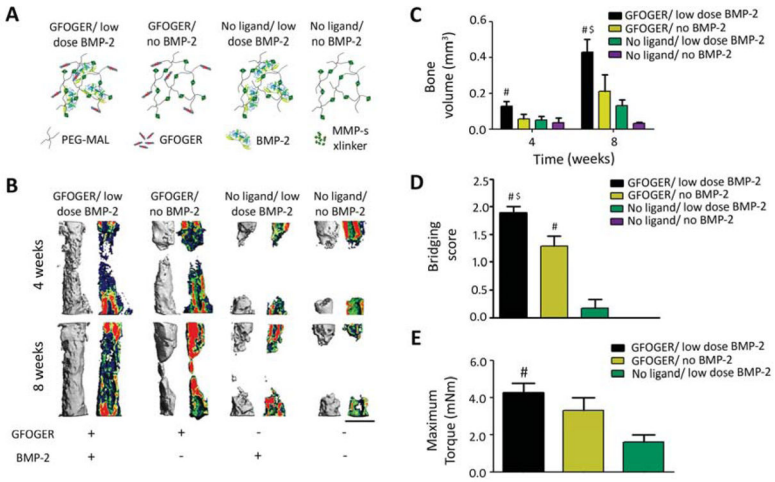

Fig. 4.

GFOGER ligand and MMP-sensitive gel degradation are crucial to bone healing in response to engineered hydrogel. (A) Cartoon of hydrogel formulations tested in this study, MMP x-linker – MMP-sensitive cross-linker. (B) 3D μCT reconstructions (left) and mineral density mappings on sagittal sections of the same defects (right), scale bar 1 mm. (C) μCT measures of bone formation at 4 and 8 weeks post-surgery. (D) Bridging scores for defects 8 weeks post-surgery. (E) Maximum torque values for radial samples 8 weeks after surgery. # $p<0.05$ compared to No ligand gels, \$$p<0.05$ compared to No ligand/BMP-2 gels. n=5 for no ligand and n=6–7 for other groups.

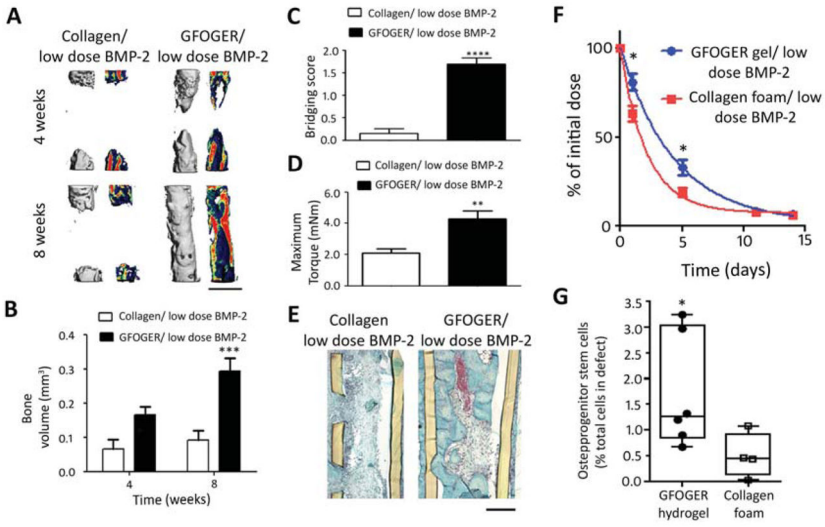

Fig. 5.

BMP-2 delivery from GFOGER-functionalized gels improves bone regeneration compared to collagen foams. (A) 3D μCT reconstructions of radii (left) and mineral density sagittal sections (right), scale bar 1 mm. (B) μCT measures of bone volume in radial defects. (C) Bridging score at 8 weeks post-implantation n=13. (D) Maximum torque values for 8 week radial samples subjected to torsion mechanical testing to failure n=5–9. (E) Sections of 8 week radial samples stained with Safranin-O/Fast Green, scale bar 200μm. (F) Retention of infrared dye-labeled BMP-2 at implanted defect site *in vivo n=6*. (G) Quantification of $CD45^{-}/CD90^{+}$ osteoprogenitor cells present in defect 7 days post implantation, n=4–6. * $p<0.05$, ***$p<0.001$ and ****$p<0.0001$ compared to Collagen foam/low dose BMP-2.